Thermo-economic analysis of a supercritical CO_2-based waste heat recovery system

Davide Bonalumi, *Antonio* Giuffrida* , and *Federico* Sicali

Politecnico di Milano – Dipartimento di Energia, Via R. Lambruschini 4, 20156 Milano, Italy

Abstract. This work investigates the performance of a supercritical CO_2 cycle as the bottoming cycle of a commercial gas turbine with 4.7 MW of electric power output. In detail, the partial heating cycle is the layout chosen for the interesting trade-off between heat recovery and cycle efficiency with a limited number of components. Single-stage radial turbomachines are selected according to the theory of similitude. In particular, the compressor is a troublesome turbomachine as it works near the critical point where significant variations of the CO_2 properties occur. Efficiency values for turbomachinery are not fixed at first glance but result from actual size and running conditions, based on flow rates, enthalpy variations as well as rotational speeds. In addition, a limit is set for the machine Mach numbers in order to avoid heavily loaded turbomachinery.
The thermodynamic study of the bottoming cycle is carried out by means of the mass and energy balance equations. A parametric analysis is carried out with particular attention to a number of specific parameters. Considering the power output calculated for the supercritical CO_2 cycle, economic calculations are also carried out and the related costs compared to those specific of organic Rankine cycles with similar power output.

1 Introduction

Supercritical CO_2 (sCO_2) power cycles are an alternative to steam bottoming cycles for natural gas combined cycle applications. Initially proposed by Feher [1] and Angelino [2] around fifty years ago, the sCO_2 power cycle has sparked an interest which is increased exponentially in the last years [3], driven by the unique features of this technology such as high thermal efficiency at intermediate temperature, small footprint and great adaptability to different energy sources. As a matter of fact, the sCO_2 power cycle is currently considered for numerous applications: concentrated solar power, nuclear reactors, oxy-combustion cycles, waste heat recovery, combined cycle power plants and many more.

Focusing on combined cycle power plants, Cho et al. [4] compared the performance of seven sCO_2 cycle layouts as bottoming power systems of the Siemens SGT5-4000F gas turbine unit with that of a steam Rankine cycle in a natural gas combined cycle power plant. A complex cascade sCO_2 Brayton cycle among the proposals presented superior efficiency in comparison with the reference steam cycle. Another comparison of sCO_2 power cycle layouts for waste heat recovery (WHR) from gas turbine was also proposed by Kim et al.

* Corresponding author: antonio.giuffrida@polimi.it

[5], though for a smaller topping cycle (5 MW). Besides the traditional layouts, the authors considered several architectures, where the partial heating cycle appeared to be an interesting solution with high potential for WHR applications. Indeed, such an architecture combines simple layout and high performance. As schematized in Fig. 1, a fraction of sCO_2 is heated by the exhaust gases in a low temperature heater in parallel with the recuperator. This solution enables a better thermal match in the recuperator and a more effective cooling of the exhaust gas from the gas turbine. According to Kim et al. [5], higher performance is always possible by complicating the sCO_2 power system with more components in the layout.

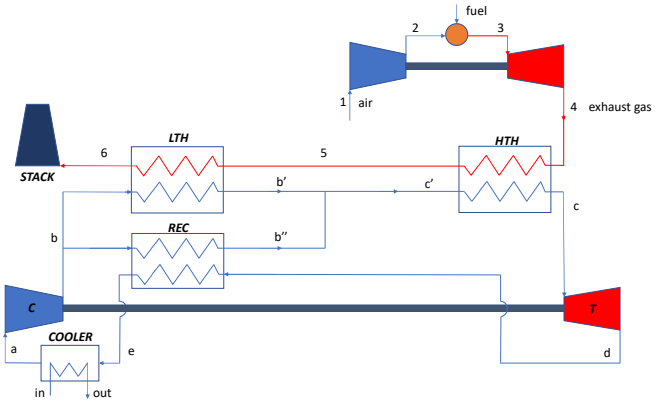

Fig. 1. Schematic lay-out of a partial heating sCO_2 cycle as bottomer of a gas turbine.

The partial heating cycle was also investigated by Wright et al. [6], who compared four cycles for waste heat recovery from a 25 MW gas turbine. The authors referred to a "preheating cycle" and highlighted that the power production is certainly higher compared to the single recuperated cycle, used as the baseline, as well as slightly greater than the one from a cascaded architecture. Differently from the above-mentioned researches [4,5], limited to thermodynamic results, Wright et al. [6] reported also economic considerations. Another work considering the partial heating cycle as a promising option due to its simple layout and limited number of components is the one carried out by Kim et al. [7], who compared the performance of the partial heating cycle (called "split flow" by the authors) against that of the single recuperated cycle for WHR from a 25 MW gas turbine. The authors evaluated the separate contributions of the cycle thermal efficiency and heat recovery effectiveness in the calculation of the total heat recovery efficiency. The performance of the partial heating cycle was found to be even better than that of a cascaded system composed of the sequence of two single recuperated cycles, in spite of the lower number of components. Other researches focusing on the partial heating cycle are present in technical literature [8,9] and the results are always consistent with the ones formerly presented [4-7].

This paper focuses on both thermodynamic and economic considerations of a partial heating sCO_2 cycle as bottoming cycle of a gas turbine. Differently from other literature works, the results of the present thermodynamic study are based on the selection of turbomachinery efficiency values according to the Aungier's suggestions for radial-type machines [10-12]. As a matter of fact, literature papers dealing with similar sCO_2 cycles assume efficiency values for compressor and turbine usually in the range 0.8-0.9, while in the current paper a mechanical matching between compressor and turbine is imposed with the shaft rotating at the same speed. An assessment of the cost of the technology is also proposed and compared with the competing organic Rankine cycle.

2 Cycle analysis and calculation assumptions

This paper investigates the sCO_2 partial heating cycle as bottoming cycle of a small-size gas turbine, whose main features are detailed in Table 1. As reported by Ishihara et al. [13], the M5A gas turbine has the best simple cycle efficiency compared to competing machines of the same output class and the exhaust gas temperature is suitable for steam generation in case of application for combined heat and power.

Table 1. Main features of the Kawasaki M5A gas turbine [13].

Electric output (kW)	4710
Heat rate (kJ/KW_{el})	11030
Thermal Efficiency	32.6%
Exhaust gas temperature (°C)	511
Exhaust mass flow (kg/s)	17.4

In the following, some considerations are included about (i) the sCO_2 conditions at compressor inlet, (ii) the mechanical matching between compressor and turbine, and (iii) basic fundamentals for a simple economic assessment of the sCO_2 cycle.

In many supercritical CO_2 cycle calculations, compressor inlet conditions are relatively near to the two-phase region, with minimum cycle temperature as low as 32°C [4,6,9,14]. As a matter of fact, lower fluid temperature at compressor inlet really reduces the compression work due to the higher fluid density near to the critical point, where the temperature is around 31°C. However, the potential for phase change in the inlet flow passages of the sCO_2 compressor should be taken into account [15-17]. Indeed, phase change could occur at the compressor inlet because of local flow acceleration and the related reduction in static pressure and temperature. Here, reference is made to Monge et al. [15], who proposed a non-dimensional criterion named Acceleration Margin to Condensation (AMC). They quantified the margin between the expected fluid properties in the inducer and the saturation line and defined the AMC as the Mach number at the throat of the impeller when the static properties of the fluid lie on the saturation line. Thus, undesired phenomena of two-phase flows are avoided if the inlet Mach number is chosen lower from the AMC. In detail, Monge et al. [15] suggested a reference value of around 0.6. Based on this figure, the minimum cycle temperature in the current work is precautionarily set at 40°C. As a matter of fact, lower values will (i) expose the compressor to the above-mentioned risks as well as (ii) require water as cooling carrier for heat rejection, which should be as cold as possible, thus limiting the applicability only to some specific geographical areas. After fixing 40°C as the sCO_2 temperature at compressor inlet, pressures in the range from the critical one (73.8 bar) to 79.8 bar and from 89.3 to 95.6 bar could be selected for an AMC value no less than 0.6. These results, as well as the following, have been calculated by means of REFPROP 9.1 [18], where the equation of state proposed by Span and Wagner [19] is implemented. This equation of state is the most accurate in the calculation of the thermodynamic properties of CO_2, which exhibits a non-linear and sharp variation near the critical point.

Turbomachinery performance strongly affects the overall cycle efficiency. In detail, this study considers a radial-inflow turbine and a centrifugal compressor, both as single-stage units. The approach suggested by Aungier [12] has been first adopted for the turbine. In order to achieve the maximum efficiency, i.e. 0.87 [12], the specific speed of the turbine is set equal to 0.55 (see Fig. 2 on the left):

$$\omega_s = \omega \cdot \frac{\sqrt{\dot{V}_{out\_is}}}{\Delta h_{is}^{0.75}} \tag{1}$$

The rotational speed of the turbine shaft results from the value of the specific speed for the fixed efficiency. As a matter of fact, after setting the maximum sCO_2 cycle temperature as well as inlet and outlet pressures for the turbine, the enthalpy drop can be quickly determined and the sCO_2 flow rate results from an energy balance at the high-temperature heat exchanger (HTH in Fig. 1). Later, the blade peripheral velocity and the rotor diameter can be calculated based on the definition of the velocity ratio:

$$VR = \frac{u_p}{\sqrt{2 \cdot \Delta h_{is}}} \tag{2}$$

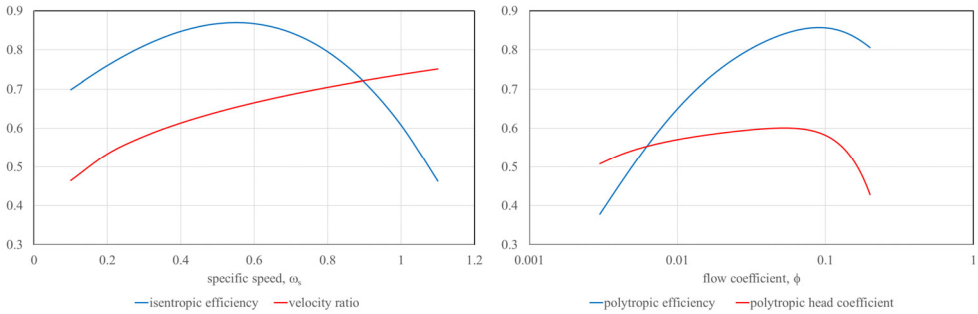

Fig. 2. Isentropic efficiency and velocity ratio of the radial-inflow turbine (on the left [12]) and polytropic efficiency and polytropic head of the centrifugal compressor (on the right [10,11]) assumed in the cycle calculations.

The rotational speed of the compressor is the same as that of the turbine as they rotate on the same shaft. Now, according to the approach by Aungier for centrifugal compressors [10,11], based on the rotational speed, inlet pressure and temperature and outlet pressure, the proper flow coefficient:

$$\phi = \frac{4 \cdot \dot{V}_{in}}{\pi \cdot D_p^2 \cdot u_p} \tag{3}$$

is set to achieve the resulting head of the compressor (see Fig. 2 on the right) and, finally, the rotor diameter of the compressor impeller.

Along with thermodynamic calculations, an economic assessment of the sCO_2 system is also caried out, based on the approach suggested by Wright et al. [5], who grouped the components into two categories: (i) turbomachinery plus auxiliary balance-of-plant (BOP) components and (ii) heat exchangers. The costs of turbomachinery plus auxiliary BOP components include turbines, compressors, seals and bearings, gear box systems, generator, motors, variable frequency drives, piping, skids, instrumentation and control systems, oil lubrication, oil cooling and purge gas management systems and CO_2 make-up systems [5]. These costs for a first-of-a-kind system were estimated as proportional to the net power production (see Table 2). It is expected that the specific cost should reduce as a production line is established.

Four heat exchangers are included in the schematic lay-out of Fig. 1. They are the high- and low-temperature heaters, the recuperator and the sCO_2 cooler. The cost of each heat exchanger is assumed to be proportional to the U·A parameter, where U is the overall heat transfer coefficient ($W \cdot m^{-2} \cdot K^{-1}$) and A is the exchange area (m^2):

$$U \cdot A = \frac{Q}{LMDT} \tag{4}$$

Q is the heat transfer rate and LMDT is the log mean temperature difference across the heat exchanger as calculated by the thermal energy balance. The non-linear trends of the thermal profiles are duly considered in order to provide a proper value for U·A. Thus, each heat exchanger is subdivided into a number of segments to calculate more precisely the temperature profiles and the overall LMDT is calculated based on Q_j and $LMDT_j$ of the single segments:

$$\frac{1}{LMDT} = \frac{1}{\mathrm{Q}} \cdot \sum_j \frac{\mathrm{Q}_j}{LMDT_j} \tag{5}$$

The specific cost for each typology of each exchanger present in the lay-out of Fig. 1 is reported in Table 2 [5].

Table 2. Cost correlations for sCO_2 power cycles originally proposed by Wright et al. [5].

Component	Specific Cost	Cost Unit
turbomachinery plus auxiliary BOP	1000	$\$\cdot kW_{el}^{-1}$
Fin tube heater	5000	$\$\cdot kW^{-1}\cdot K$
Recuperator	2500	$\$\cdot kW^{-1}\cdot K$
Shell-and-tube sCO_2 cooler	1700	$\$\cdot kW^{-1}\cdot K$

Based on the component costs, a specific figure in $\$\cdot kW_{el}^{-1}$ results for each sCO_2 bottoming cycle calculation. A comparison with a competing technology, namely the organic Rankine cycle (ORC), formerly investigated by Carcasci et al. [20] as a suitable solution for waste heat recovery from gas turbines, is made according to the specific cost suggested by Baldasso et al. [21]:

$$SC_{ORC} = 19358 \cdot P_{el}^{-0.2703} \tag{6}$$

after retrieving the cost estimations reported by Lemmens [22]. In the former relation, SC_{ORC} is the specific cost of the ORC technology in $\$\cdot kW_{el}^{-1}$ and P_{el} is the net electric power production in kW_{el}.

3 Results

This section presents the results of the partial heating cycle as bottomer of the Kawasaki M5A gas turbine.

A first analysis has been carried out after setting the maximum sCO_2 pressure at 280 bar, consistently with the work of Cho et al. [4] and the recuperator effectiveness equal to 90%. As anticipated, the turbine isentropic efficiency is fixed equal to 87%, whereas the compressor efficiency results from the turbomachinery matching for the same rotational speed. The temperature difference on the cold side of the high-temperature heater (HTH in Fig. 1) is imposed to be equal to 20°C in order to limit its effectiveness at values less than 95%. As previously introduced, the minimum sCO_2 cycle temperature is always 40°C and two ranges for the minimum pressure have been considered to achieve an AMC value at the compressor inlet no less than 0.6. Then, the net power production of the sCO_2 cycle has

been maximized by properly setting the turbine inlet temperature and the sCO_2 mass split fraction at the compressor outlet.

The results in Fig. 3 are obtained for the four possible architectures of the centrifugal compressor, considering both open and covered impellers, as well as vaned and vaneless diffuser. After looking at the net electric power results in Fig. 3, a clear trend with limited variations despite the architecture of the compressor can be appreciated. The highest value of the net electric power is possible when selecting the highest value of the inlet compressor pressure in the investigated range. In this case, the compression ratio is the lowest and equal to 2.93. Based on these results, the best solution seems to be the one where the compressor has an open impeller and a vaned diffuser. However, after setting the minimum sCO_2 cycle pressure, really slight variations in power output can be appreciated. As a matter of fact, even in the case the compressor has covered impeller and vaneless diffuser, power reductions of ≈ 45 kW at 95.6 bar or ≈ 70 kW at 74 bar are calculated, compared to the case with the maximum power output.

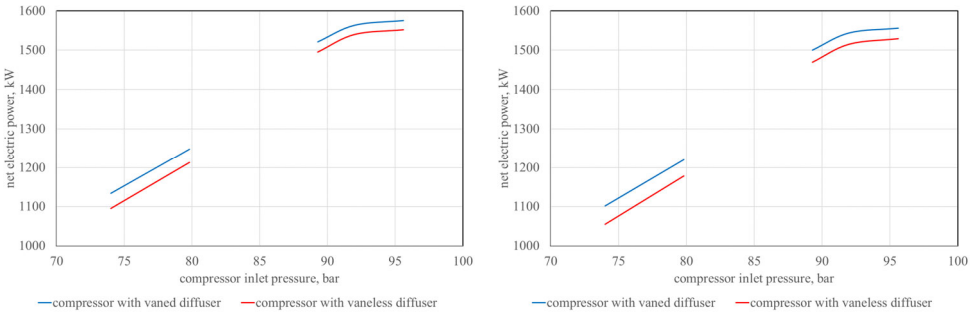

Fig. 3. Net electric power output from the sCO_2 cycle as a function of the minimum fluid pressure. The compressor has an open impeller (on the left) and a covered impeller (on the right), respectively.

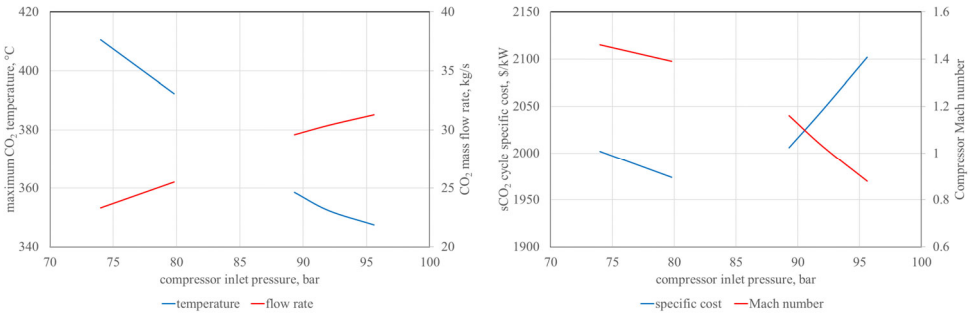

Fig. 4. Maximum cycle temperature, CO_2 mass flow rate, specific cost and compressor Mach number as functions of the minimum fluid pressure when adopting a compressor with open impeller and vaned diffuser.

Other specific results are shown in Fig. 4, limiting the analysis to the power cycle where the compressor has an open impeller and a vaned diffuser. In detail, Fig. 4 on the left shows that the lower the sCO_2 pressure at compressor inlet, the higher the sCO_2 temperature at turbine inlet as well as the lower the mass flow rate calculated from the energy balance at the high-temperature heater. This result is consistent with the one reported by Kim et al. [7], where a maximum sCO_2 cycle temperature far from the exhaust gas temperature at the topping cycle has been anticipated. Looking at Fig. 4 on the right, slight variations have been calculated for the specific cost, but the other result requires more attention. The compressor Mach number is calculated as the ratio between the impeller peripheral speed and the speed of sound of the fluid at compressor inlet. Actually, single-stage architectures

are supposed for the turbomachinery in this study and, if the minimum sCO_2 pressure is too low, the compressor is heavily loaded. Indeed, the range between 74 and 79.8 bar results in an excessively high compressor Mach number compared to the value of around 1.25 suggested by Modekurti et al. [23] for a single stage compressor. Nevertheless, a lower value of 0.86 for the compressor Mach number is reported in recent researches by Romei et al. [24,25], studying an highly loaded centrifugal compressor for sCO_2 applications operating in near-critical conditions. Thus, looking at the results in Fig. 4 on the right, only the case with the sCO_2 minimum pressure at 95.6 bar seems to be feasible because of the lower machine Mach number (0.88). Limited to this case, a specific cost of 2102 $/kW is really interesting when compared to 2646 $/kW as the result of Eq. (6) for the ORC technology.

Removing the former assumption of 280 bar as the maximum sCO_2 pressure and calculating the corresponding value based on a fixed compressor Mach number, another analysis has been carried out for three values of this parameter, namely 0.75, 0.8 and 0.85, the latter supposed to be a reasonable value based on the above-mentioned researches [24,25]. In addition, minimum temperature and pressure of the sCO_2 cycle are fixed parameters: the first is always fixed at 40°C and the second is selected inside the two above-mentioned ranges (74-79.8 and 89.3-95.6 bar).

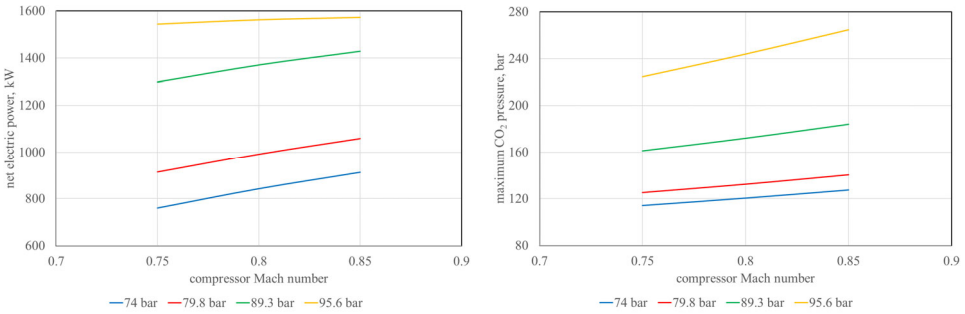

Fig. 5. Net electric power output from the sCO_2 cycle (on the left) and maximum cycle pressure (on the right) depending on the compressor Mach number and on the minimum cycle pressure.

In detail, referring to the boundary values of the two ranges for the minimum cycle pressure, Fig. 5 on the left reports the net electric power, which is almost constant in case of minimum sCO_2 pressure at 95.6 bar despite of the compressor Mach number. Actually, the lower the sCO_2 pressure at compressor inlet, the lower the maximum cycle pressure for a given compressor Mach number, i.e. a fixed load for the compression unit. Once again, more interesting sCO_2 cycle performance results are achieved when the sCO_2 pressure at compressor inlet is selected in the range 89.3 to 95.6 bar. In particular, the upper limit is preferable for a lower specific cost. As a matter of fact, in case of sCO_2 pressure at 95.6 bar, the specific cost moves from 2535 to 2165 $/kW, when increasing the compressor Mach number. In detail, the highest cost is justified by calculations of the low-temperature heater resulting in higher effectiveness then higher UA value: the lowest cost is really similar to the one (2102 $/kW) previously calculated in case of maximum sCO_2 pressure of 280 bar and compressor Mach number of 0.88.

Other results are reported in Fig. 6 as regards the turbomachinery matching. The higher the minimum cycle pressure and the higher the turbomachinery rotational speed. In addition, the rotational speed increases with the compressor Mach number: the maximum calculated value is ≈ 53000 rpm, which is lower compared to the rotational speed of the Sandia National Laboratories system designed to operate at 75000 rpm. Focusing on the case of minimum sCO_2 pressure at 95.6 bar, Fig. 6 also reports turbine and compressor rotor diameters as the result of the fixed compressor Mach number.

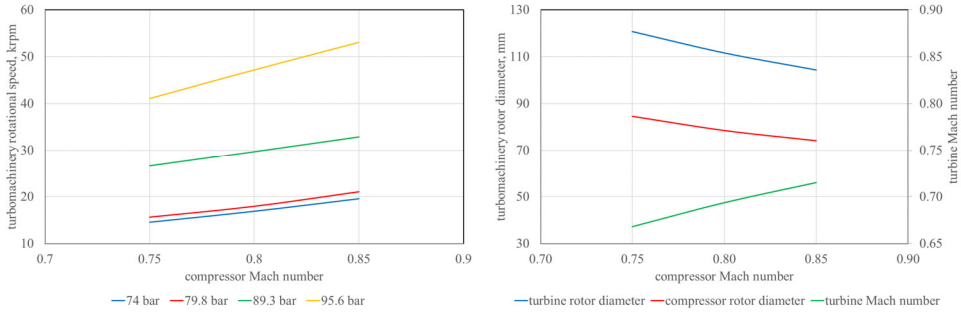

Fig. 6. Turbomachinery rotational speed depending on the compressor Mach number and the minimum cycle pressure (on the left) and turbomachinery rotor diameters with turbine Mach number (on the right) depending on the compressor Mach number (minimum sCO_2 pressure equal to 95.6 bar)

Actually, higher rotational speeds play a role in reducing the turbomachinery size, and a larger rotor is calculated for the turbine compared to the compressor. The turbine Mach number increases with the head at the compressor. This is mainly due to the higher peripheral speed of the turbine blade. As a matter of fact, the latter becomes higher as the compressor Mach number increases since it is calculated as the product between the velocity ratio, which does not change because of the turbine specific speed fixed to 0.55 (see both Eq. (2) and Fig. 2), and the spouting velocity which depends on the square root of the isentropic enthalpy drop.

Paying attention to the heat transfer between gas and sCO_2 at both HTH and LTH, the T-Q diagrams of the two primary heaters are reported in Fig. 7, limited to the case of a compressor Mach number fixed at 0.85.

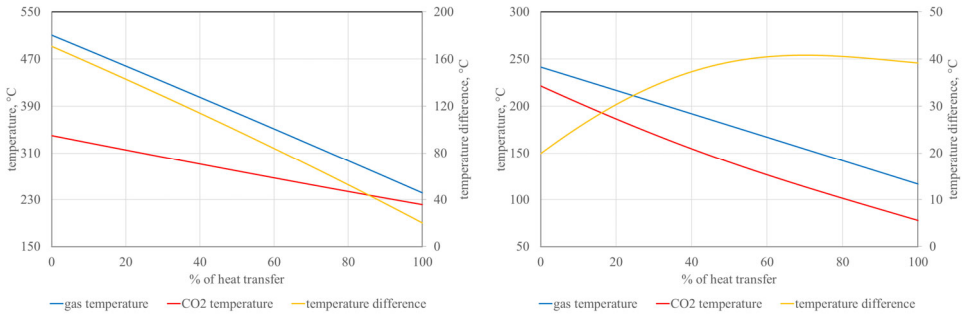

Fig. 7. T-Q diagram of the HTH (on the left) and of the LTH (on the right) in case of minimum cycle pressure equal to 95.6 bar and compressor Mach number equal to 0.85

In detail, the thermal power exchanged by the HTH (around 5200 kW) is more important than the one at the LTH (around 2300 kW) as the latter does not process the total sCO_2 flow rate but only a fraction (around 27%). The sCO_2 temperature profile is not linear in the LTH due to the significant variations of the thermodynamic properties of the fluid at lower temperatures. The minimum temperature difference (20°C) occurs at the hot side of the heat exchanger and rises inside it. On the other hand, the sCO_2 temperature profile in the HTH is quite linear as well as the temperature difference, with its minimum value (20°C) at the cold side of the HTH.

Ultimately, Fig. 8 reports the trends of thermodynamic efficiency, heat recovery efficiency and total efficiency depending on the compressor Mach number. The temperature of the gas exiting the stack is included as well. The higher the aerodynamic load of the compressor, the warmer the sCO_2 flow rate at the inlet of the LTH, the higher the temperature of the gas at the stack. In detail, the heat recovery efficiency decreases as

the compressor Mach number rises. In case of lower compressor Mach numbers, the stack temperature approaches 80°C, hence it is not convenient to set compressor Mach numbers less than 0.75. Fig. 8 also details the total efficiency results almost constant, similarly to the net electric power production anticipated in Fig. 5.

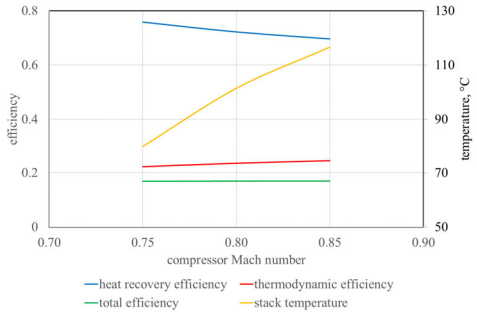

Fig. 8. Heat recovery efficiency, thermodynamic efficiency, total efficiency and gas temperature at the stack depending on the compressor Mach number (minimum cycle pressure equal to 95.6 bar)

4 Conclusions

This paper has investigated the performance of a supercritical CO_2 partial heating cycle as the bottomer in a combined cycle where the topper is a small gas turbine with 4.7 MW of electric power output. The proposed supercritical CO_2 cycle effectively combines heat recovery and cycle efficiency with a limited number of components.

After setting an upper limit for the Mach number of the single-stage centrifugal compressor, i.e. a specific compression load, the thermodynamic analysis suggests around 1.6 MW_{el} for the power output from the supercritical CO_2 cycle and the economic assessment returns a specific cost of around 2100 $/kW, which is a lower value compared with the competing ORC technology.

Future developments of this work will be oriented to investigations of other architectures of supercritical CO_2 cycle for waste heat recovery applications, in order to assess possible improvements in terms of power output and cost of the power system.

References

1. E. Feher, Energy Conversion and Management **8** (1968)
2. G. Angelino, Journal of Engineering for Power **90**, 3 (1968)
3. A. Yu, W. Su, X. Lin, N. Zhou, Nuclear Engineering and Technology **53** (2021), DOI: 10.1016/j.net.2020.08.005
4. S.K. Cho, M. Kim, S. Baik, J.I. Lee, Investigation of the bottoming cycle for high efficiency combined cycle gas turbine system with supercritical carbon dioxide power cycle, in Proceedings of ASME Turbo Expo 2015, DOI: 10.1115/GT2015-43077
5. M.S. Kim, Y. Ahn, B. Kim, J.I. Lee, Energy **111** (2016), DOI: 10.1016/j.energy.2016.06.014
6. S.A. Wright, C.S. Davidson, W.O. Scammell, Thermo-economic analysis of four sCO_2 waste heat recovery power systems, in Proceedings of 5th International Symposium on Supercritical CO_2 Power Cycles, 2016
7. Y.M. Kim, J.L. Sohn, E.S. Yoon, Energy **118** (2017), DOI: 10.1016/j.energy.2016.10.106

8. E.D. Sanchez Villafana, J.P. Vargas Machuca Bueno, Applied Thermal Engineering **152**, 1 (2019), DOI: 10.1016/j.applthermaleng.2019.02.052
9. B. Li, S.S. Wang, K. Wang, L. Song, Energy Conversion and Management **228** (2021), DOI: 10.1016/j.enconman.2020.113670
10. R. H. Aungier, Centrifugal compressor stage preliminary design and component sizing, in Proceedings of the ASME 1995 International Gas Turbine and Aero Engine Congress and Exposition, DOI: 10.1115/95-GT-078
11. R.H. Aungier, *Centrifugal compressors - A strategy for aerodynamic design and analysis*, ASME Press, 2000
12. R.H. Aungier, *Turbine aerodynamics - Axial-flow and radial-inflow turbine design and analysis*, ASME Press, 2005
13. S. Ishihara, K. Terauchi, T. Ikeguchi, M. Ryu, Development of high efficiency 5 MW class gas turbine the Kawasaki M5A, In Proceedings of ASME Turbo Expo 2019, DOI: 10.1115/GT2019-90773
14. D. Thanganadar, F. Asfand, K. Patchigolla, Applied Energy **255** (2019) DOI: 10.1016/j.apenergy.2019.113836
15. B. Monje, D. Sanchez, M. Savill, P. Pilidis, T. Sanchez, A design strategy for supercritical CO_2 compressors, in Proceedings of ASME Turbo Expo 2014, DOI: 10.1115/GT2014-25151
16. B. Monge, D. Sánchez, M. Savill, T. Sánchez, Exploring the design space of the sCO_2 power cycle compressor, in Proceedings of the 4th International Symposium on Supercritical CO_2 Power Cycles, 2014
17. T.C. Allison, A. McClung, Limiting inlet conditions for phase change avoidance in supercritical CO_2 compressors, in Proceedings of ASME Turbo Expo 2019, DOI: 10.1115/GT2019-90409
18. E.W. Lemmon, M.L. Huber, M.O. McLinden, NIST Standard Reference Database 23: Reference Fluid Thermodynamic and Transport Properties-REFPROP, Version 9.1
19. R. Span, W. Wagner, J. Phys. Chem. Ref. Data **25**, 6 (1996), DOI: 10.1063/1.555991
20. C. Carcasci, R. Ferraro, E. Miliotti, Energy **65** (2014), DOI: 10.1016/j.energy.2013.11.080
21. E. Baldasso, M.E. Mondejar, U. Larsen, F. Haglind, Energies **13** (2020), DOI: 10.3390/en13061378
22. S. Lemmens, Energies **9** (2016), DOI: 10.3390/en9070485
23. S. Modekurti, J. Eslick, B. Omell, D. Bhattacharyya, D. C. Miller, S. E. Zitney, International Journal of Greenhouse Gas Control **62** (2017), DOI: 10.1016/j.ijggc.2017.03.009
24. A. Romei, P. Gaetani, G. Persico, Design and off-design analysis of a highly loaded centrifugal compressor for sCO_2 applications operating in near-critical conditions, in Proceedings of the 4th European sCO_2 Conference for Energy Systems, 2021, DOI: 10.17185/duepublico/73969
25. A. Romei, P. Gaetani, G. Persico, On sCO_2 compressor performance maps at variable intake thermodynamic conditions, in Proceedings of ASME Turbo Expo 2021